

Optical Figure Inspection of Diamond-Turned Metal Mirrors

R. N. Shagam, R. E. Sladky,* and J. C. Wyant

Optical Sciences Center
University of Arizona
Tucson, Arizona 85721

Abstract

This paper demonstrates that the optical testing of diamond-turned surfaces is best accomplished by interferometry and not by tests which measure wavefront slope. Certain conditions regarding the interferometer configuration must be met in order to generate meaningful and accurate interferograms. A 40 cm diameter aperture modified Mach-Zehnder interferometer mounted directly on the diamond-turning lathe to facilitate rapid testing of figure between fabrication cuts is described. Results for a spherical surface tested in a Twyman-Green interferometer and an off-axis parabola tested in the Mach-Zehnder interferometer are illustrated.

Introduction

The diamond-turning development program at the Oak Ridge Y-12 Plant (operated by Union Carbide Corporation under contract with USERDA) is currently involved in the fabrication of copper plated mirrors for the CO₂ laser fusion experiments being conducted at Los Alamos Scientific Laboratories (LASL). These mirrors — long-radius spheres being fabricated on the Moore diamond-turning lathe and short-focus off-axis parabolas being fabricated on the Excello lathe, must be inspected and certified for figure accuracy prior to delivery. While these mirrors are to be used at infrared wavelengths, testing at visible wavelengths has proved both convenient and invaluable by using conventional laser interferometry. Non-interferometric methods^{1,2} for qualifying surface figure have been used; however, they are more difficult to implement and less interpretable than direct interferometry. The nature of the diamond-turned surface does place restrictions on the test configuration used. These requirements are:

- (1) Single pass null test
- (2) Record of complete surface test
- (3) Insensitivity to steep zonal slopes on surface
- (4) Sharp in-focus image of mirror surface formed on recording plane.

These conditions are met by the Twyman-Green interferometer for testing spherical surfaces and by a modified Mach-Zehnder configuration for testing off-axis parabolas.

Nature of Surface Errors in Diamond Turned Surfaces

In principle, diamond-turned optical components could be tested using any of the techniques applied to conventionally processed optics if it were not for the presence of sharp zonal irregularities in the machined surfaces. These zones, which under visual examination suggest the appearance of a phonograph record, are due principally to errors in the radial path traced by the diamond tool across the surface. Contours such as parabolas which require a motion of the tool having two degrees of freedom, in general, exhibit more pronounced zones than do those surfaces such as flats which require a motion of the tool having only one degree of freedom.³ These zones, which may have little adverse effects on the performance of an optical system at infrared wavelengths, can seriously impair certain types of optical tests performed at visible wavelengths owing to the scale of

the defect relative to the wavelength of the incident radiation.

Errors in the surface may be divided into three categories based upon the lateral scale of the deviation;⁴ surface figure, surface finish or roughness, and surface waviness. Surface figure is the principal quantity which affects the gross image forming characteristics of an optical system and is represented by surface height variations having a lateral separation or wavelength on the order of centimeters and a vertical amplitude on the order of fractions of a micron to several microns. Figure errors may be due to a number of factors, including low order tool path errors, machine setup errors, spindle growth and dynamic flexures of the mirror part during machining, as well as faulty fixturing which can produce a warped or astigmatic part.

Surface finish or roughness is a measure of the short period variations in surface height and is the property which generates large angle scatter in an optical system as well as increased surface absorption. Having a lateral separation of less than a millimeter and surface height variations less than approximately 500Å, roughness is a function of such parameters as tool feed rate, machinability of the substrate, residual vibrations in the lathe, and diamond tool quality.

Lying between the two extremes is surface waviness, which is responsible for low angle scatter, and additional degradation of the optical image. It is manifest in the form of the jagged radial zones seen in diamond turned surfaces. Waviness has a lateral separation on the order of millimeters and an amplitude approaching fractions of a micron. Waviness can be attributed to short period straightness and angular errors in the machine slide ways and lead screw which are amplified by the so-called Abbe' offsets of the tool relative to the slide and are outside of the servo loop controlling carriage positions.

Optical Testing Techniques

While conventionally processed optical surfaces suffer from figure error, waviness and roughness, the nature of the defects have such a low order compared to the wavelength of visible light that a surface may be evaluated by any number of traditional optical tests, including geometric slope tests such as the Foucault⁵ or Hartmann⁶ tests, or by direct wavefront measuring interferometry as with the laser Twyman-Green interferometer. In contrast, diamond-turned surfaces are not well suited to geometric slope tests owing to the extreme waviness of the surface manifested as steep sloped zones having a short lateral width. However, interferometric surface measurements are possible provided the waviness has an amplitude less than the interferometric fringe spacing and provided the interferogram recording plane is an in-focus image of the optical surface. Also possible are, of course, interferometric tests performed at effective infrared wavelengths by using either a direct infrared interferometer or by using two-wavelength holographic interferometry.⁷ Either technique, however, is costly or complicated and inconvenient and is unnecessary if the above two criteria can be met.

The Foucault class of tests fail because rather than measuring the surface profile directly, one measures the slope, or derivative, of the surface, and as such, is a noisy process. In the transverse knife edge test or its geometric equivalent, the transverse wire test,⁸ one records the transverse knife edge position in the image plane as a function of the position of its shadow projected on the mirror surface. Alternately, in the more common but

*Union Carbide Corp., Y-12 USERDA Facility, Oak Ridge, Tenn. 37830.

equivalent longitudinal knife edge or wire tests, one records the position of focal positions of zones on the mirror surface. In the presence of many narrow steep zones having the same slope it becomes difficult to locate a single shadow on the mirror corresponding to a given slope on the surface, thus making an accurate reconstruction of the surface profile by integration impossible. Furthermore, the surface may suffer from a discontinuity in surface height in which, although the slopes on either side of the discontinuity are the same, the surface heights are different. Consequently, a surface phase error can go undetected because the discontinuity is thought to be a local zone rather than a step height change.

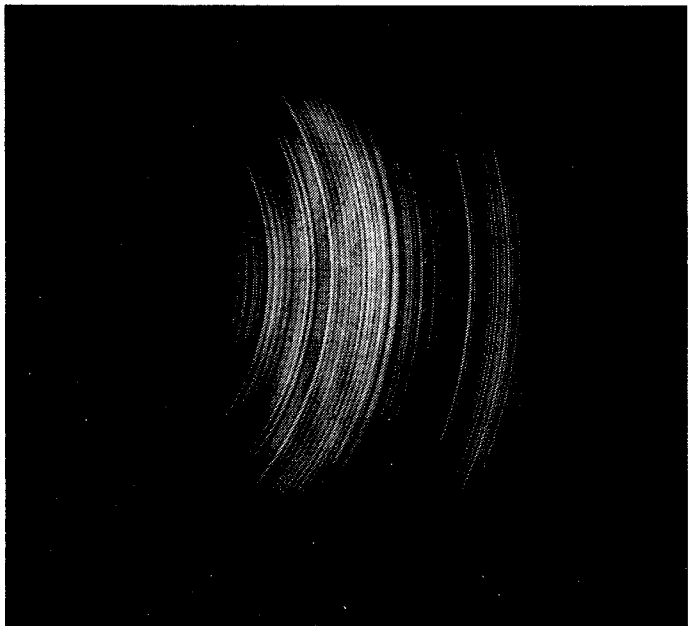


Figure 1. Foucaultgram of a diamond turned surface. The surface is an off-axis portion of a sphere fabricated on a Moore diamond-turning lathe.

Figure 1 shows a Foucaultgram of a 20 cm diameter off-axis section of a diamond-turned sphere having a 339.8 cm radius of curvature and diameter of 39 cm which was produced on a Moore diamond-turning lathe. Note the presence of a number of narrow zones due to waviness in addition to the two broad zones due to figure error. The heights of these narrow zones cannot be quantitatively measured from Foucault test data.

The Ronchi test, which in effect simultaneously records the positions of the shadows of equally spaced transverse wires as in the wire test, also fails because it is a slope test. Each wire in the Ronchi grating maps a shadow corresponding to the locus of constant slope. Thus, one records overlapping loci which, upon data reduction, become uninterpretable. Figure 2 is a Ronchi-gram of the same mirror as before.

Another disadvantage of the Foucault class of tests is that they can measure surface profile readily only in one direction, whereas one needs an effective test for astigmatism due to improper fixturing during machining. The Hartmann test, in which a screen having an array of small apertures is placed over the mirror surface to generate a real ray trace of the system by photographically recording the positions of the rays in the region near the caustic to yield slope error, will generate surface error data for the entire surface. However, because the surface is sampled only at discrete locations, one knows nothing about the surface in the regions between the sample points. Furthermore, as in the Foucault test, the Hartmann test cannot measure discontinuities in the surface.

Also to be considered is the effect of the Hartmann screen hole size. If too large a hole is used, then the light can be reflected off a large number of zones, possibly giving the image at the

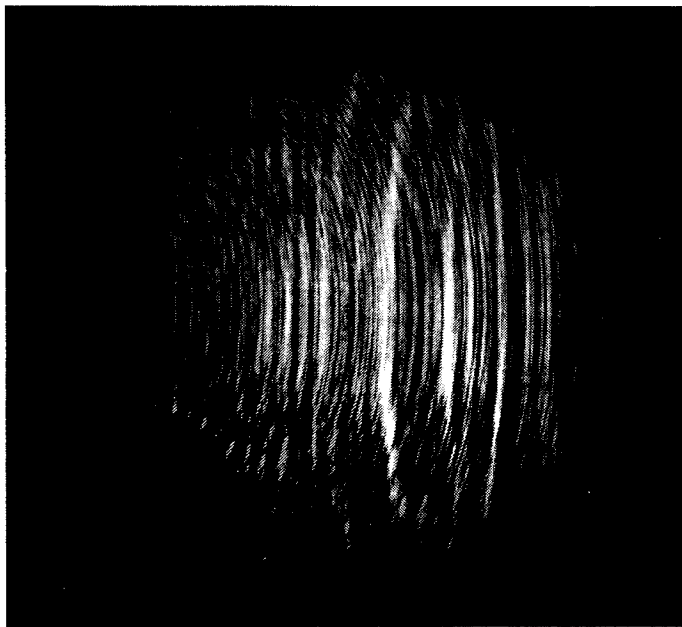


Figure 2. Ronchi-gram of the same surface. Grating frequency is 200 lines/inch and has been defocused sufficiently to accentuate the overlap of Ronchi zones.

photographic plate a complicated shape for which the centroid will be difficult to locate. Too small a hole, and only the slope of a given zone that is not representative of the surrounding region may be measured instead.

Direct wavefront measuring interferometry avoids the problem encountered in slope tests as applied to diamond-turned optics in that a record of the entire surface is made at once and that surface error rather than slope error is recorded directly. By introducing a suitable amount of tilt between the wavefront from the surface and the reference wavefront, a set of interference fringes is superimposed over the image of the optical surface. These fringes represent loci of constant optical path difference. Departure from straightness of a fringe is thus directly related to variations in surface height.

An interferometer must still meet certain requirements in order to perform satisfactorily. One is that the interferogram recording plane must be a sharp in-focus conjugate image to the mirror surface in order to give a proper representation of the height variations. Because of Fresnel diffraction, the out-of-focus image of a pure phase object contains intensity variations, whereas the in-focus image does not. As shown in Figure 3, the zones in a diamond-turned mirror yield concentric rings in the out-of-focus image of the surface. The rings disappear when the image is focused, as in Figure 4. When the reference beam from the interferometer is introduced in the interference fringes superimposed over the in-focus image as shown in Figures 7 and 8 are much more finely detailed than those on the out-of-focus images shown in Figures 5 and 6. The shapes of the zones are quite apparent in the in-focus interferograms. Note especially how the fringes become difficult to locate when they run parallel to the zones in the out-of-focus image.

The origin of the zonal intensity variations is demonstrated in Figure 9. Let S and S' be the surface and in-focus image of the surface, respectively. Z is a zone having slope different from the rest of the mirror. Consequently, the wavefront from that zone is reflected at an angle different from the rest of the reflected wavefront. From geometric optics we can show that points A' , Z' , and B' in image plane S' are separate images of points A , Z , and B in object plane S regardless of the directions in which the wavefronts from those points traveled. Consequently, A' , Z' , and B' do not interfere with one another and there are no intensity variations. However, in planes I and O , which

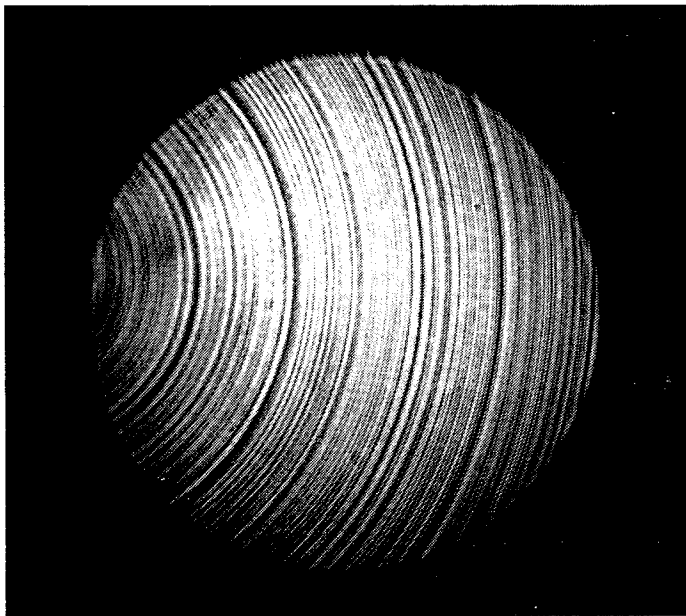


Figure 3. Out-of-focus image of diamond-turned surface. Ring structure is due to Fresnel diffraction from diamond turned zones.

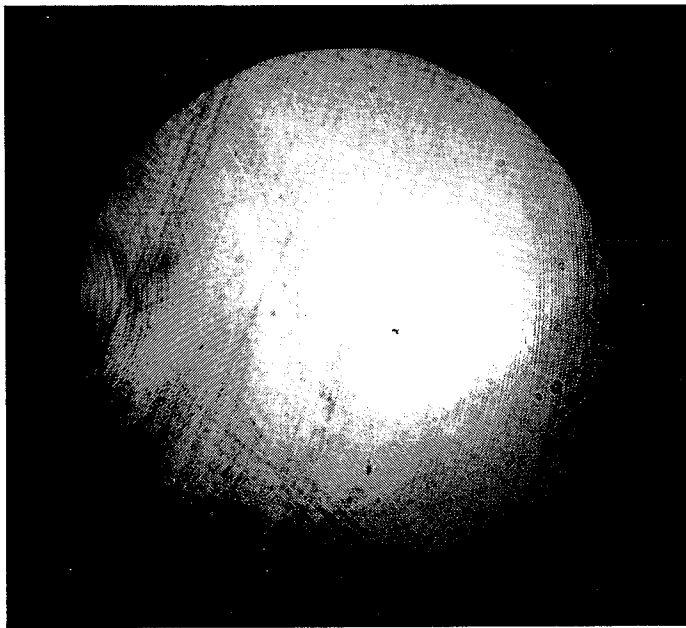


Figure 4. In-focus image of same surface. Ring structure has vanished.

are inside or outside the Gaussian image plane, the wavefronts from points A and Z, and from B and Z, interfere at points $A'Z'$ and $B'Z'$, respectively.

Because of the requirement of a sharp focus of the mirror surface, the double-pass testing of a surface should be avoided unless the surface can be imaged back onto itself. For example, in the traditional method for testing a parabola by autocollimation off a reference flat, two images of the mirror surface are formed in different planes and it is not possible to obtain a sharp focus for both images simultaneously. Consequently fringe detail is blurred. In addition, the wavefront can reflect off a steep zone on one part of the mirror at an angle, reflect off the autocollimating flat, and return to the mirror at a slightly shifted location, thus contributing an erroneous amount to the wavefront in the form of a ghost zone at that portion of the mirror. Figure 10 illustrates this principle.

Double-pass testing might be avoided for a second reason —

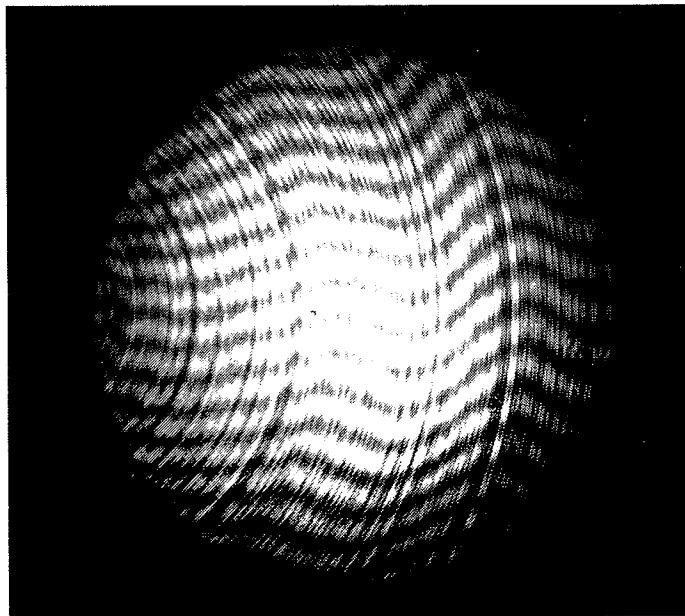


Figure 5. Interferogram of out-of-focus surface. Interference fringes are perpendicular to zones. Shape and amplitude of zones is immeasurable and mirror edge is ill-defined.

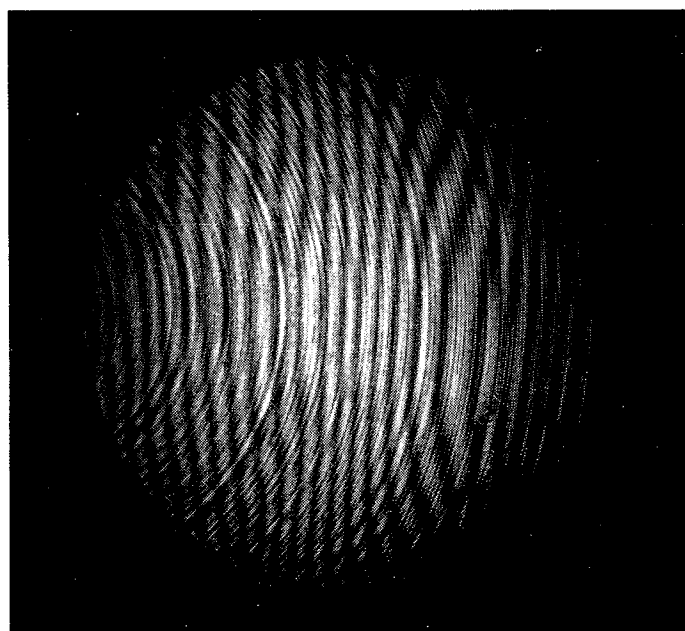


Figure 6. Interferogram of out-of-focus surface. Interference fringes are parallel to zones and are difficult to locate.

increased sensitivity. If the amplitude of the surface waviness exceeds an amount greater than one fringe spacing, fringes from adjacent orders interlace and appear to blend together. Consequently, if the surface waviness is already marginal for a single-pass test, then a double-pass configuration will increase the problem.

As with conventional optical surfaces, interferometric testing of diamond-turned optics is best accomplished if the test is performed in a null configuration. In this case, contour errors are simple departure from straightness of interference fringes. In a non-null configuration, it is necessary to mathematically subtract out the aberration introduced by the arrangement. However, if the expected aberration is too great to subtract mathematically, it may usually be subtracted out optically with an Offner null lens¹⁰ or a computer generated hologram.¹¹ In the

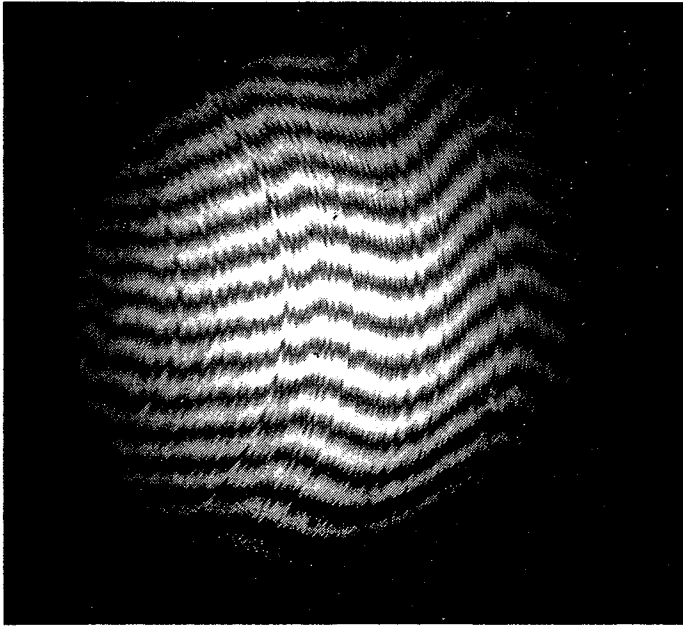


Figure 7. Interferogram of in-focus surface. Fringes are perpendicular to zones. Shape and amplitude of zones are easily measured from fringe contour and mirror edge is easily discerned.

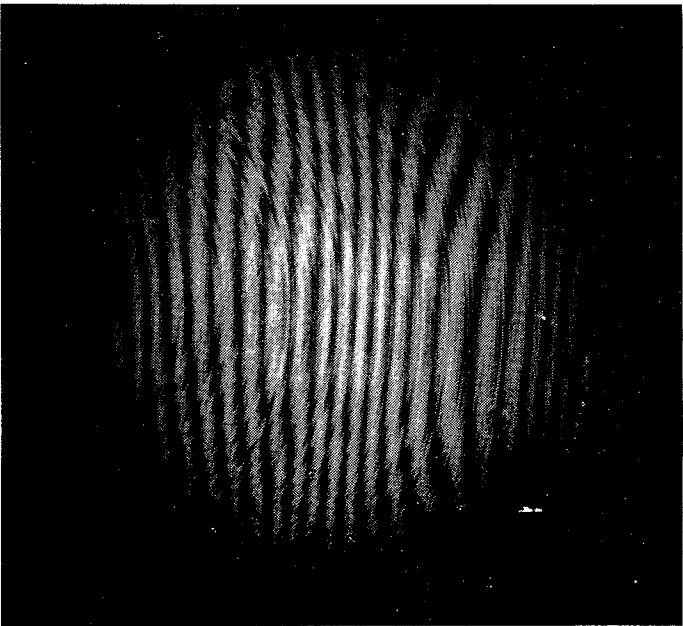


Figure 8. Interferogram of in-focus surface. Fringes are parallel to zones but are easy to locate.

testing of specialized aspherics, the simplest null test can be obtained by combining simple null lenses and computer generated holograms.

Description of On Machine Mach-Zehnder Interferometer

The interferometer that satisfies the requirements of a single-pass null test for the testing of off-axis parabolas is the modified Mach-Zehnder configuration as shown schematically in Figure 11, and as shown installed on the cross slide of the Excello diamond turning lathe in Figure 12. A 2 mw HeNe laser beam is expanded and diverged to illuminate a 43 cm diameter $f/4$ plano-convex aspheric collimator lens, fabricated by the Optical Sciences Center, University of Arizona. The optic axis is aligned parallel to the axis of rotation of the spindle of the lathe.

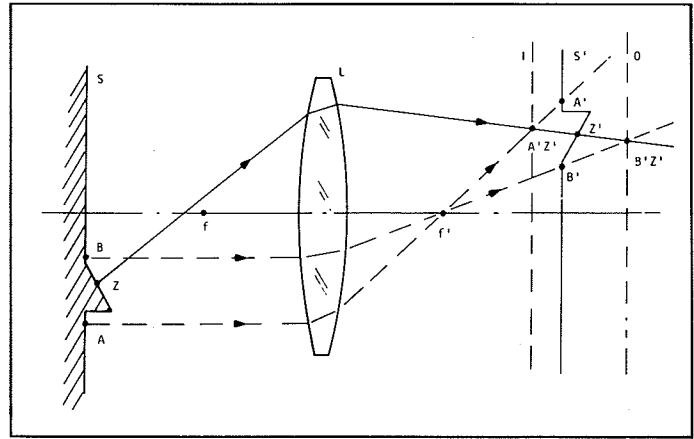


Figure 9. Generation of intensity variations in out-of-focus image of mirror surface.

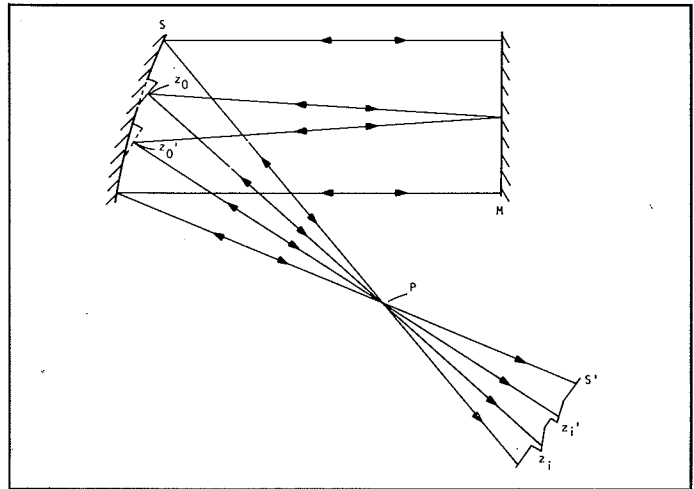


Figure 10. Generation of ghost zones in testing a parabola by autocollimation. P = illuminating point source, S = mirror surface, S' = image of surface, M = autocollimating flat. Z_0 = zone on mirror, Z_0' = reflection of Z_0 onto back of surface. Z_1 and Z_1' = images of Z_0 and Z_0' .

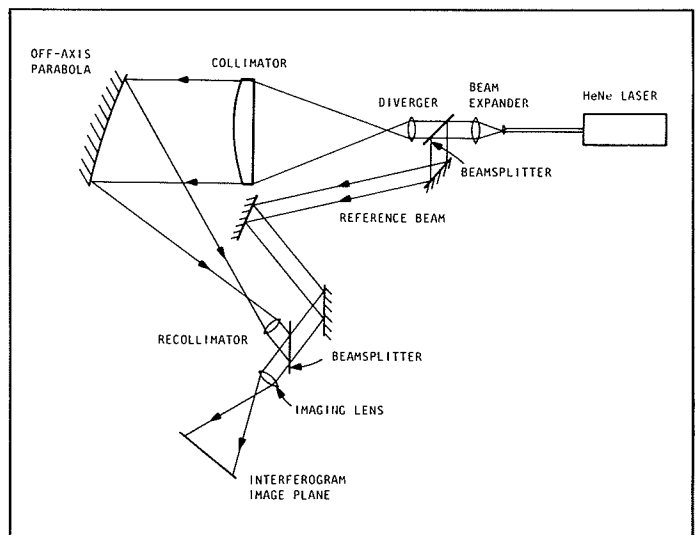


Figure 11. Modified Mach-Zehnder interferometer schematic.

Mounted on the spindle is the parent fixture into which are potted six off-axis parabolic mirror segments. Each of these parabolas, which have a vertex focal length of 77.27 cm, are 40.64 cm

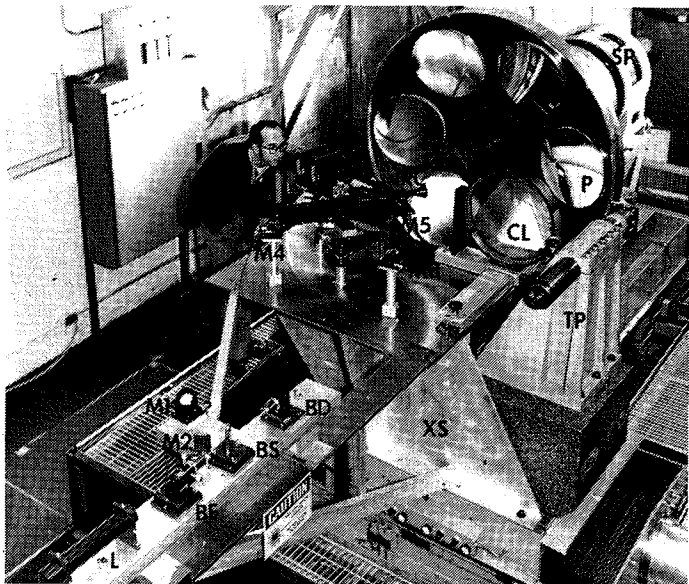


Figure 12. Modified Mach-Zehnder interferometer as installed on Ex-cello diamond turning lathe. L = laser, BE = beam expander, BS = beam-splitter, BD = beam diverger, CL = collimator lens, P = off-axis parabola under test, RC = recollimating lens, M1-M5 = reference beam turning mirrors, PC = recording camera, XS = lathe x-slide carriage, TP = tool post supporting diamond tool, SP = lathe spindle head.

in diameter and positioned 48.56 cm from the spindle axis. The wavefront from a parabola under test is focused to a point and recollimated by a 2.5 cm focal length lens. The collimated reference beam is split off from the first beam expander and combined with the wavefront from the parabola. The mirror pupil with the superimposed interference fringes is imaged onto the film plane of a Polaroid MP-4 camera using an 82 mm focal length lens. The front end of a Tinsley Laboratories laser Twyman-Green interferometer provides the recollimating and beam combining optics.

An alignment procedure has been developed that insures that the interferometer is collimated and aligned parallel to 2.5 arc seconds of the spindle axis. The collimator and beam diverger lenses are removed from the system and the x-slide carriage is positioned so that the collimated light from the beam expander is pointed at the spindle axis on which is mounted an optical flat supported by a two-axis tilt mount. By placing a precision corner cube reflector in the reference arm of the interferometer to reflect the beam back upon itself through the first beamsplitter, the interferometer is now operating in a Twyman-Green mode. Looking at the fringes generated by the interference of the reference beam and the reflection off the spindle mirror, both the spindle mirror and the fixture supporting the laser beam expander and beamsplitter are tilted until there is just one broad fringe seen across the field of view that remains stationary with spindle rotation. In front of the position of the collimator lens is placed a 40 cm diameter optical flat which is aligned parallel to the spindle flat by autocollimation. The collimator lens is now installed and the plano rear surface of the lens is also made parallel to the spindle flat. The beam diverger is now installed and its focal and lateral positions relative to the collimator lens are established again by autocollimation. The large flat and corner cube are now removed and the x-slide repositioned so that the off-axis parabola is now illuminated by the collimator. The Tinsley interferometer is now positioned at the focus of the parabola and the reference beam adjusted to generate interference fringes in the interference plane.

Testing of Spherical Mirrors

The concave spherical mirrors being fabricated for LASL have

a diameter of 40 cm and radius of curvature in the vicinity of 1300 cm. These mirrors are fabricated on a Moore diamond-turning lathe and inspected off the machine owing to the relative ease with which they may be removed from or replaced on the supporting fixture if need be. As spheres present no particular testing problems when examined at the center of curvature in a laser Twyman-Green interferometer, the testing procedure will not be discussed.

Analysis of Interferograms

The resulting interferograms are interpreted by both visual inspection and by computer analysis. Visual inspection will quickly reveal whether the overall quality of the part is at least marginally acceptable. Excessive waviness as well as such in-process errors such as a tool slippage during machining can be rapidly identified in this manner. Once the visual inspection proves satisfactory, a computer analysis is performed to quantify contour or figure errors which could have been due to such errors as machine instability, faulty fixturing or an incorrect numerical control tape and to certify that the mirror does meet specifications. Thus, provided the errors are systematic and not statistical, a new numerical control tape can be prepared from the resultant analysis.

Visually satisfactory interferograms of each mirror are manually scanned with a coordinate digitizer coupled to a Hewlett-Packard 9830 calculator. Fringe data is recorded in the form of fringe order number and (x,y) pupil coordinates for up to 400 data points approximately equally spaced across the pupil. The data is analyzed by the computer program FRINGE,¹² which was developed by John Loomis of the Optical Sciences Center, University of Arizona. FRINGE fits the data to a 36-term Zernike polynomial using the Gram-Schmidt method of least-squares fitting. The output of the program is in the form of a contour map of the resulting wavefront as well as statistical characterization of the wavefront. Also available are geometric and diffraction analyses of the image plane for evaluation of system performance at any desired wavelength.

The interferogram analysis cannot take into account the effect of surface waviness because the data is digitally filtered by the processes of sampling the surface at discrete locations and fitting the data to a polynomial. Thus only the low order figure error and its effect upon image formation can be calculated. However, because the interferogram can record the surface waviness, it should be possible to extend the prediction of the system performance to incorporate surface scatter using an appropriate scatter theory based upon knowledge of the surface structure.

Results

Figure 13 shows an interferogram of an off-axis parabola after an initial evaluation cut made on the Ex-cello lathe. The interferogram, while revealing a surface figure of unacceptable quality, demonstrates the importance of having an interferometric on-machine inspection capability. In this instance, not only is it apparent that the outer edge of the mirror is turned down, but that the mirror figure is too wavy. These errors have been attributed, in part, to thermal instabilities in the diamond-turning lathe. The magnitude of these defects could not be measured by visual observation, and would be prohibitively time consuming and expensive to measure by removing a mirror from the fixture and testing it off the machine. The Y-12 diamond turning engineers have used this interferogram to diagnose machine faults and initiate corrective measures.

The interferogram of a typical Moore turned sphere is shown in Figure 14, and the contour map from the resulting FRINGE analysis in Figure 15. The rms figure error of this example was .151 microns, and peak to valley figure error was .850 microns. The contour map reveals a four-pole symmetry in the surface figure. This was attributed to distortion introduced by the four

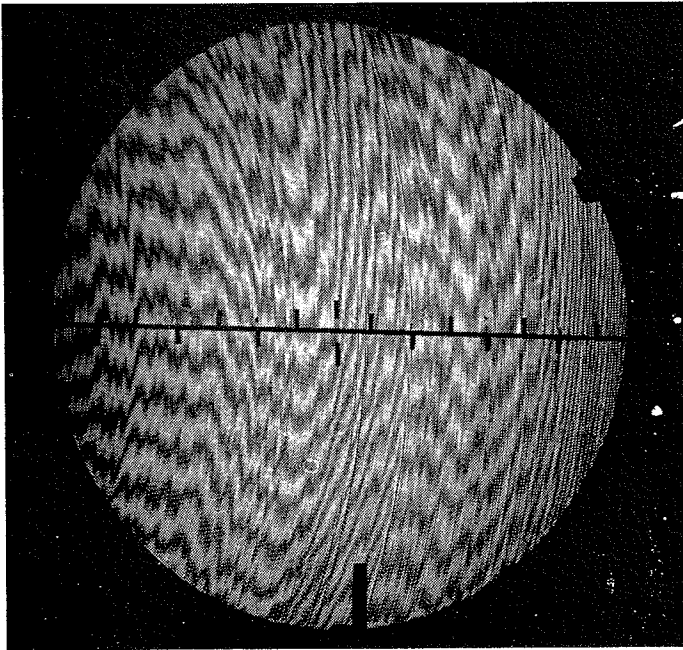


Figure 13. Mach-Zehnder interferogram of preliminary cut of off-axis parabola. This interferogram has proved to be a valuable diagnostic tool in correction of machine deficiencies.

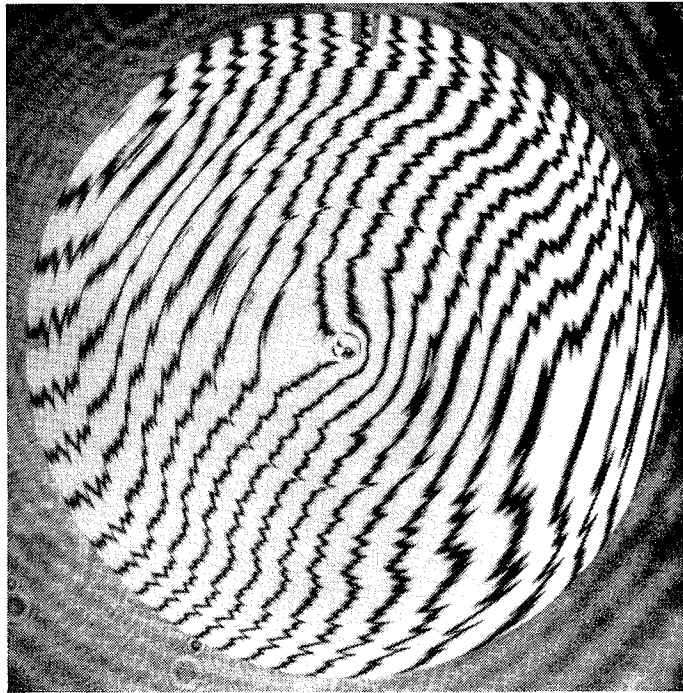


Figure 14. Laser Twyman-Green interferogram of Moore-turned spherical mirror. Diameter = 40 cm, radius of curvature = 1320 cm.

clamps fixturing the mirror to the spindle. More recent diamond-turning efforts have resulted in a reduction in astigmatism once this problem had been identified from interferometric data.

Summary

Diamond-turned optics can best be tested for figure at visible wavelengths using conventional interferometry provided that the optical surface is properly imaged onto the interferogram plane. Interferometry has proved itself valuable in the diagnosis

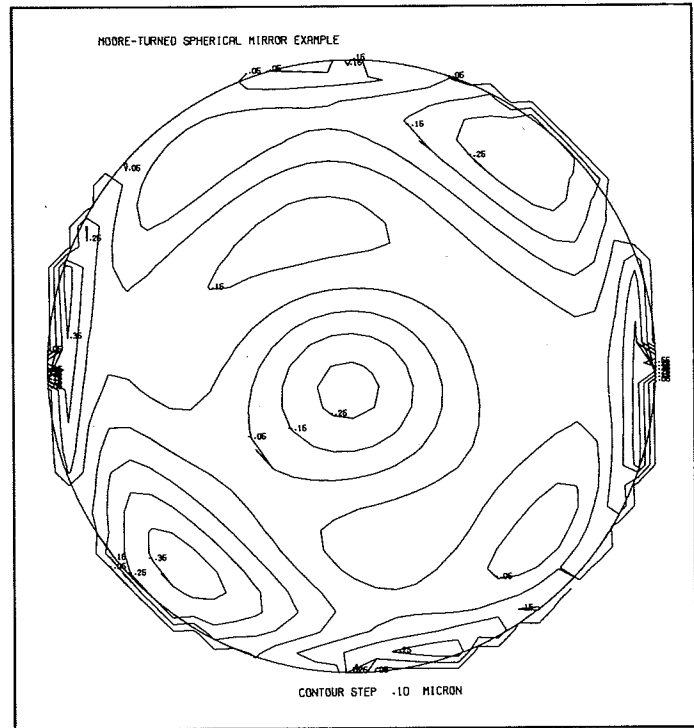


Figure 15. Contour map from FRINGE analysis of Moore-turned sphere. Contour intervals are .1 microns in surface height variations.

of fabrication errors and improvement of figure quality of diamond turned optics.

Acknowledgments

The authors wish to thank Howard Gerth, Richard Dean and Jack Brown for their assistance in the design and implementation of the Mach-Zehnder interferometer. This work was supported in part by LASL under contract NP6-46285-1.

References

1. J. E. Sollid, R. E. Sladky, W. H. Reichelt, and S. Singer, "Single-Point Diamond-Turned Copper Mirrors: Figure Evaluation," *Appl. Opt.* **15**, 1656 (1976).
2. R. E. Sladky and R. H. Dean, "Optical Measurements of Surface Quality and Figure of Diamond-Turned Mirrors." Document Y-DA-6328, Union Carbide Corporation, Oak Ridge, Tennessee, Dec. 12, 1975.
3. T. T. Saito, "Machining of Optics: An Introduction," *Appl. Opt.* **14**, 1773 (1975).
4. J. M. Bennett, "Measurement of the RMS Roughness, Autocovariance Function and Other Statistical Properties of Optical Surfaces Using a FEKO Scanning Interferometer," *Appl. Opt.* **15**, 2705 (1976).
5. L. Foucault, "Memoire sur la Construction des Telescopes en Vene Argente," *Ann. Obs. Imp. Paris* **5**, 197 (1859).
6. I. Ghozeil and J. E. Simmons, "Screen Test for Large Mirrors," *Appl. Opt.* **13**, 1773 (1974).
7. J. C. Wyant, "Testing Aspherics Using Two Wavelength Holography," *Appl. Opt.* **10**, 2113 (1971).
8. R. Platzek and E. Gaviola, "On the Errors of Testing and a New Method of Surveying Optical Surface and Systems," *J. Opt. Soc. Am.* **29**, 484 (1939).
9. V. Ronchi, "Forty Years of History of a Grating Interferometer," *Appl. Opt.* **3**, 437 (1964).
10. A. Offner, "A Null Corrector for Paraboloidal Mirrors," *Appl. Opt.* **2**, 153 (1963).
11. A. J. MacGovern and J. C. Wyant, "Computer Generated Holograms for Testing Optical Elements," *Appl. Opt.* **10**, 619 (1971).
12. J. S. Loomis, "Analysis of Interferometric Data for the Multiple Mirror Telescope: Optics." *J. Opt. Soc. Am.* **66**, 1116 (1976). ☺